Heliyon 10 (2024) e31576

Contents lists available at ScienceDirect

Heliyon

journal homepage: www.cell.com/heliyon

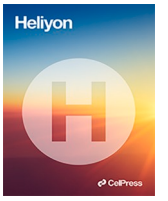

Research article

Impact of chitosan extracted from shrimp shells on the shrinkage and mechanical properties of cement-based composites using dendritic fibrous nanosilica

Liyuan Zhao [a,**], Man Wang [b], Liwei Zhang [a], Seyed Mohsen Sadeghzadeh [c,d,*]

[a] School of Civil Engineering and Architecture, XinXiang University, XinXiang, 453003, China
[b] School of Civil and Architectural Engineering, Zhengzhou University of Science and Technology, Zhengzhou, 450064, China
[c] Department of chemistry, Neyshabur Branch, Islamic Azad University, Neyshabur, Iran
[d] New Materials Technology and Processing Research Center, Neyshabur Branch, Islamic Azad University, Neyshabur, Iran

ARTICLE INFO

Keywords:
Nanoparticle
Chitosan
Cement
Cement-based composites
Interfacial stretching potency
Autogenous shrinkage

ABSTRACT

Dendritic fibrous nanosilica (DFNS) was functionalized using microcrystalline chitosan, derived from shrimp exoskeletons, to act as a robust anchor, resulting in DFNS@Chitosan. In order to prevent the restacking of chitosan sheets, the supramolecular polymerized chitosan not only served as a spacer but was also incorporated into cement-based composites. The physical-chemical characteristics of DFNS@Chitosan were assessed through various analytical techniques such as TEM, SEM, TGA, FTIR, AFM, XPS, and EDX. The potency and auto-induced contraction of Cement-based composite materials fortified with DFNS@Chitosan were probed. The incorporation of DFNS@Chitosan resulted in an increase in both compressive and interfacial stretching potency of the cement-based composites. Furthermore, the presence of DFNS@Chitosan effectively inhibited the occurrence of auto-induced contraction in the cement-based paste. This research endeavor is anticipated to promote an alternative utilization of DFNS and shrimp waste shells in the development of sustainable building materials.

1. Introduction

Immunization of valuable metals and nanoparticles onto various minerals and polymers has been reported as a method for preparing heterogeneous catalysts [1–6]. The utilization of chitosan (CS) as a natural polymer has been employed in the field of green chemistry due to its advantageous characteristics including biodegradability, non-toxicity, biocompatibility, high surface area, and cost-effectiveness [7–10]. Chitosan is derived from chitin, which is the second most abundant natural polymer after cellulose and can be found in organisms such as fungi, shrimps, insects, and crabs [11]. They serve as excellent ligands for supporting ions of nickel, cerium, rhodium, ruthenium, copper, and other transition metals owing to their inability to dissolve in organic solvents and the existence of amino groups that can be functionalized in their morphology [12–15]. The incorporation of metal complexes supported by chitosan has proven successful in various catalytic reactions such as Suzuki, oxidation, Heck reactions, and hydrogenation [16–18].

* Corresponding author. Department of Chemistry, Neyshabur Branch, Islamic Azad University, Neyshabur, Iran.
** Corresponding author.
E-mail addresses: zly_jbgsn@sina.com (L. Zhao), M.sadeghzadeh@iau-neyshabur.ac.ir, Seyedmohsen.sadeghzadeh@gmail.com (S.M. Sadeghzadeh).

https://doi.org/10.1016/j.heliyon.2024.e31576
Received 21 February 2024; Received in revised form 12 April 2024; Accepted 19 May 2024
Available online 21 May 2024

Furthermore, to enhance catalytic efficiency, hybrid materials of silica have been synthesized with diverse structures, including silica beads, hierarchical porous materials, and composite membranes [19–21].

Lately, the discovery of dendritic fibrous nanosilica by Polshettiwar et al. [22–24] has garnered attention. This material has demonstrated remarkable efficacy in various domains, including gas absorption, sensors, biomedical applications, solar-energy harvesting, energy storage, and catalysis. In our main report [25–28], it was referred to as fibrous nanosilica (KCC-1) due to its fibrous structure. However, it is worth noting that the fibers possess a thickness ranging from 3.5 to 5.2 nm, leading to the adoption of diverse nomenclature in the literature, such as dandelion, dendritic, fibrous, lamellar, nanoflower, and wrinkled.

The concept of environmentally friendly, low-carbon development has emerged as a prominent global research subject. This concept entails addressing the conflict between the escalating demand for infrastructure and the imperative to mitigate environmental issues, including greenhouse gas emissions and the depletion of finite resources. As a major industry characterized by substantial energy consumption and reliance on natural resources, the creation of cement has long been a focal point for energy preservation and emission minimization efforts [29,30]. Consequently, the endeavor for eco-friendly cement and concrete has become the foundation of the modern construction industry's transformation and upgrading. One crucial approach to achieving eco-friendliness and sustainability in concrete lies in reducing cement usage and substituting it with industrial and agricultural waste materials [31,32]. In addition to benefiting the natural environment, this facilitates the recyclable utilization of non-renewable resources and emissions of detrimental substances. Due to our ongoing focus on nanoparticle development, a new approach has been described for creating specific nanocomposites by altering chitosan, a natural material, and using a solution extracted from shrimp shells. This is aimed at advancing the industrial application of chitosan. In this study, chitosan was obtained from shrimp shells, combined with fibrous DFNS, and then introduced into cement-based composites (as shown in Scheme 1). The study measured the physical characteristics and auto-induced contraction of the cement-based composites that integrated both treated and untreated chitosan extracted from shrimp shells.

2. Experimental

2.1. The procedure for preparing DFNS NPs

Initially, 3.2 g of TEOS was added to a blend of 26 mL cyclohexane and 2.2 mL 1-pentanol. Then, an agitated blend of 0.6 g urea and 1 g cetylpyridinium bromide (CPB) in 30 mL of water was introduced. The amalgamation was agitated continuously for 37 min at 28 °C, then was put in a Teflon-lined hydrothermal vessel and subjected to a temperature of 120 °C for 6.5 h. The collected silica was eliminated using centrifugation, rinsed with deionized water and acetone, and dried in a drying chamber. Finally, the material was calcined at 550 °C for 5 h in air.

2.2. The procedure for preparing DFNS@Chitosan NPs

Water (16 mL) and DFNS (1.3 mmol) were combined in a flask, and then acetic acid (0.68 mL) was introduced using ultrasonication. Chitosan (160 mg) was included at ambient temperature and agitated for an additional 11 h at 75 °C. The final substances were collected, rinsed with ethanol and deionized water in sequence, and then vacuum dried at 85 °C for 1.7 h.

The process of preparing DFNS@Chitosan reinforced cement-based composites.

The preparation of DFNS@Chitosan reinforced cement-based composites involved the design of three kinds of matrix frameworks. Type A consisted of plain cement without the introduction of DFNS@Chitosan. Type B was fiber-cement with the addition of 2.0 wt% of DFNS. Type C was fiber-slag-cement with the introduction of 2.0 wt% DFNS@Chitosan. The content of DFNS@Chitosan was consistently maintained at 2.0 wt% of the binder.

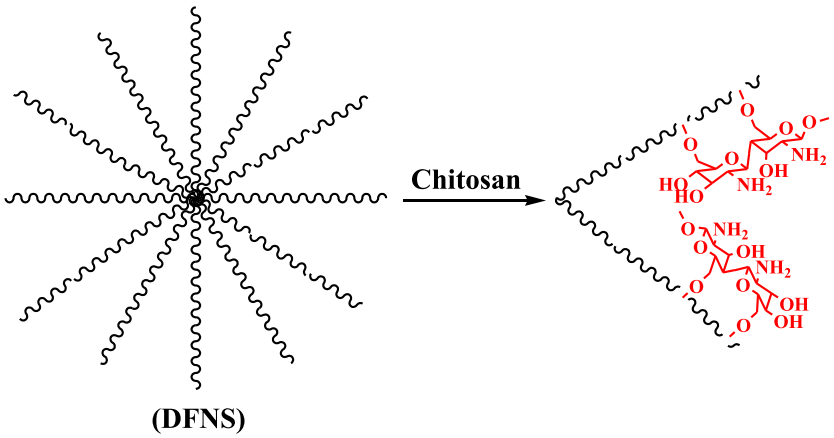

Scheme 1. A visual representation of creating DFNS@Chitosan.

3. Results and discussion

The initial phase in achieving this nanoparticle design involved the functionalization of DFNS with chitosan groups, which could serve as pseudo chelators or ligands affecting the physical and contraction characteristics of cement-based composites. This functionalization was accomplished through the alteration after the synthesis of the DFNS fibers by reacting them with chitosan to create DFNS@Chitosan (as illustrated in Scheme 1).

The SEM and TEM techniques were employed to characterize the structures and morphologies of both the DFNS and DFNS@Chitosan NPs. In Fig. 1a, the TEM image of the DFNS samples revealed uniform spheres with a diameter of 390 nm and well-defined textures, along with wrinkled fibers of about 14 nm thickness arranged in a 3D configuration from the center after growth, and open pores conically formed using radial structures. The SEM image in Fig. 1c illustrates the solid fiber nature of the entire sphere, facilitating increased access to active surfaces and mass transfer of reactants through the open channels of the hierarchical fiber structure. TEM and FESEM images of DFNS@Chitosan NPs indicated that the morphology of DFNS remained unchanged after modification (Fig. 1b and d). Thermogravimetric analysis of the material at various temperatures confirmed the thermal stability of DFNS@Chitosan nanoparticles (refer to Fig. 2). Weight reduction at 160 °C was attributed to the removal of both chemisorbed and physisorbed solvents on the surface of the DFNS. Organic weight reductions (in the range of 200–410 °C) of DFNS@Chitosan NPs were found to be 27.3 %, confirming the presence of organic structures supported on the DFNS surface. The reactions were further analyzed using FTIR. The band at 1080 cm^{-1} corresponds to the vibration of the O–Si bonds for unmodified DFNS. Two bands at 3016 and 2974 cm^{-1}, related to H–C stretching, significantly increased after the polymerized chitosan was applied to the surface of DFNS. Additionally, Fig. 3 shows two new bands at 1564 and 1492 cm^{-1}, corresponding to H–C and C–C stretching, respectively.

The surface roughness of the NPs was assessed using AFM (atomic force microscopy) analysis. In Fig. 4, the topographic representation revealed that the brighter yellowish-white areas, indicating higher elevations, increased with a reduction in T/W, suggesting an augmentation in the irregularity of the catalyst's outer layer. This analysis confirms the fibrous structure of this nanoparticle. XPS was employed to investigate the chemical composition at the level of DFNS@Chitosan NPs. Fig. 5 presents an XPS schematic of the collected catalyst, displaying peaks for Si, C, O, and N, with the presence of N 1s further confirming the functionalization of DFNS with chitosan. This confirms the presence of chitosan in the nanoparticles. The elemental composition of the catalyst was determined by EDX analysis, as depicted in Fig. 6, revealing the presence of nitrogen, silicon, oxygen, and carbon in the DFNS@Chitosan NPs.

Influence of spherical DFNS nanoparticles and chitosan (DFNS@Chitosan NPs) on the durability of cement mortar. Fig. 7 displays the crushing potency and the stretching potency of the cement-based mortars at three distinct stages of curing: 5, 15, and 30 days. As

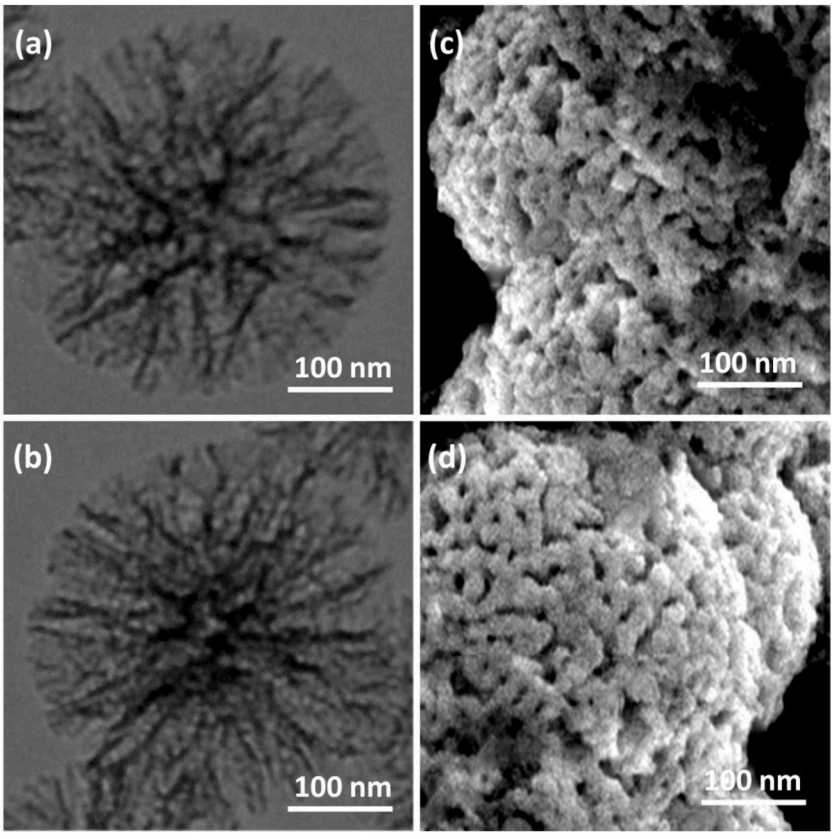

Fig. 1. TEM illustrations of DFNS NPs (a); and DFNS@Chitosan NPs (b); FESEM images of DFNS NPs (c); and DFNS@Chitosan NPs (d).

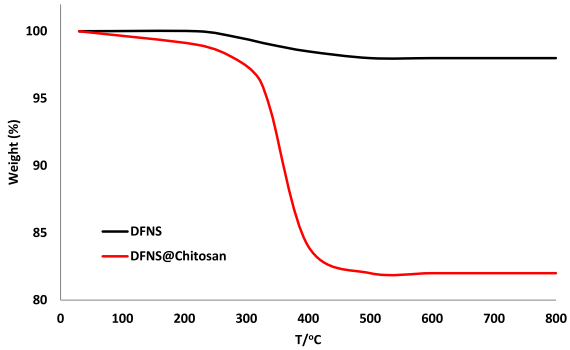

Fig. 2. Thermogravimetric analysis (TGA) plot of the various constituents of the catalyst.

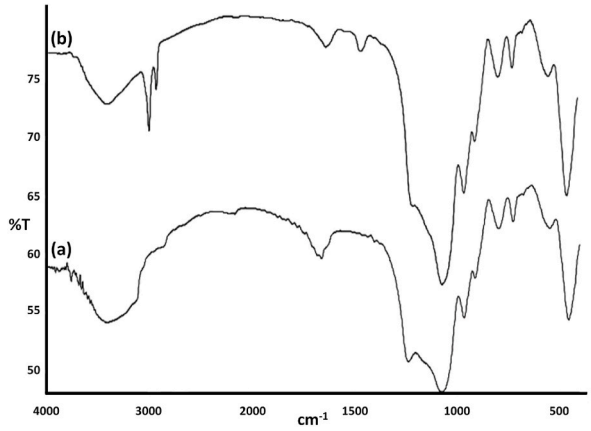

Fig. 3. FTIR spectra of DFNS (a), and DFNS@Chitosan (b).

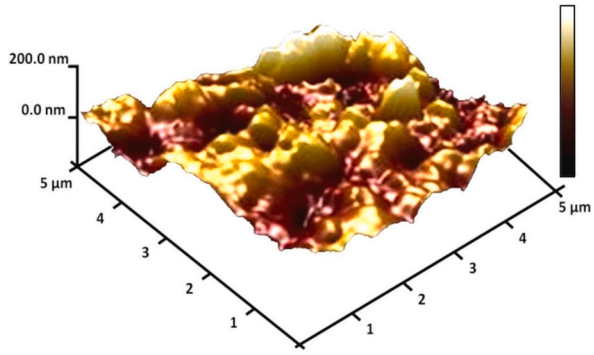

Fig. 4. Three-dimensional AFM images of DFNS@Chitosan.

expected, the load-bearing capacity of the cement-based mortars gradually decreased as the DFNS@Chitosan NPs content increased for each age. Specifically, the load-bearing capacity of the mortars at 5, 15, and 30 days decreased by 34.3 %, 32.0 %, and 40.0 %, respectively, as the DFNS@Chitosan NPs content increased up to 3 %. This reduction in potency can be attributed to the uneven dispersion of the DFNS@Chitosan NPs in the cement matrix, leading to a higher number of empty spaces. Additionally, with the increase in DFNS@Chitosan NPs content, the cohesion between the DFNS@Chitosan NPs and mortar diminished, resulting in increased porosity and a subsequent significant reduction in compressive potency.

Fig. 8 depicts the correlation between DFNS@Chitosan content and interfacial stretching potency at various curing ages. It is evident that the inclusion of DFNS@Chitosan significantly influenced the interfacial stretching potency of cement mortars. The interfacial stretching potency rose with the rise in DFNS@Chitosan content from 0 to 2.0 %. Nevertheless, a further increase in

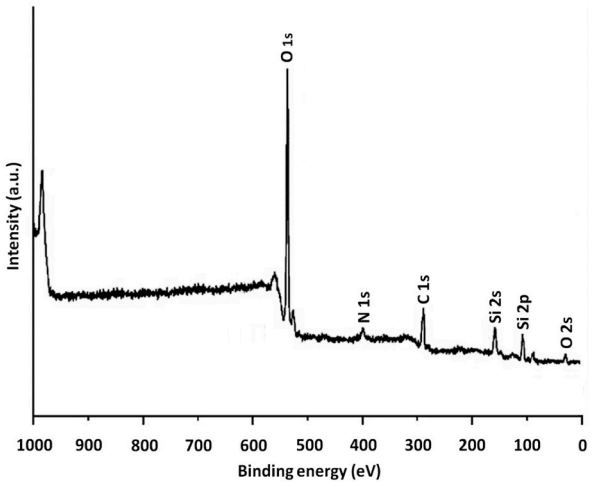

Fig. 5. XPS data for DFNS@Chitosan.

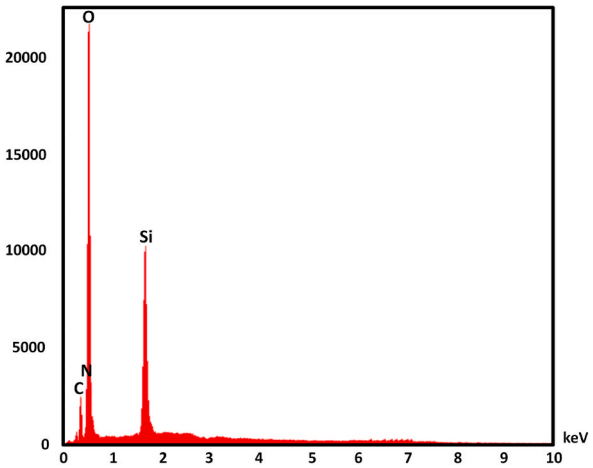

Fig. 6. EDX spectra of DFNS@Chitosan.

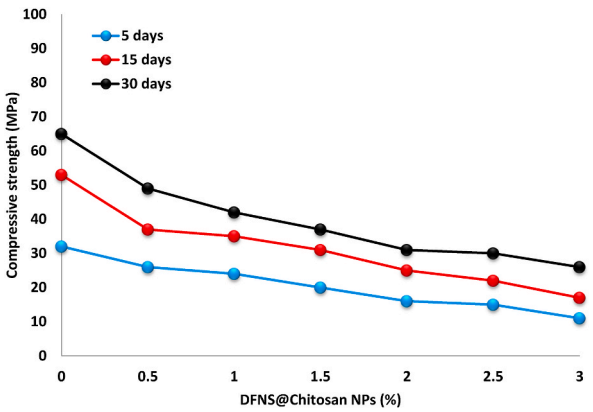

Fig. 7. Ramifications of DFNS@Chitosan NPs content on the compressive potency.

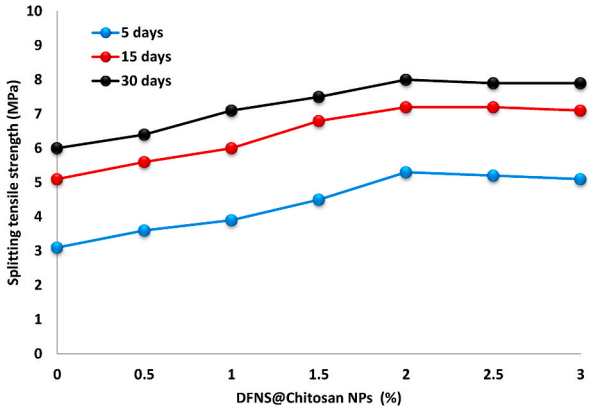

Fig. 8. Ramifications of DFNS@Chitosan NPs content on the interfacial stretching potency.

DFNS@Chitosan content from 2.0 % to 3.0 % led to a drop overall. Based on these findings, an optimal DFNS@Chitosan content of 2.0 % was selected for designing the cement-based mixture. The addition of 2.0 % DFNS@Chitosan enhanced the interfacial stretching potency of the cement-based mortars. DFNS@Chitosan contributes to bearing a specific stretching force due to its restricted movement within the cement-based matrix. Nevertheless, with DFNS@Chitosan addition surpassing 2 %, the interfacial strength of the mortars tended to decrease, potentially due to increased carbohydrate dissolution, hindering cement hydration and strength development.

The ramification of pretreated DFNS@Chitosan on the potency of cement-based mortar. Fig. 9 displays the load-bearing capacity of cement-based mortars after 5, 15, and 30 days of curing. The mortar without DFNS or DFNS@Chitosan served as a point of comparison. It is evident that the mortars containing DFNS@Chitosan exhibited higher load-bearing capacity than the reference. The addition of DFNS and DFNS@Chitosan in cement-based mortar resulted in reduced porosity and increased compressive potency. Compared to the mortar without DFNS or DFNS@Chitosan, the mortar containing DFNS showed an increased load-bearing capacity of 18.7 %, 26.4 %, and 13.8 % at 5, 15, and 30 days, respectively. Chitosan support on the DFNS surface added to the potency enhancement by producing a rough surface that enhanced the intermeshing action among the DFNS@Chitosan and the cement-based substrate. At 5, 15, and 30 days, the DFNS@Chitosan mixed mortars exhibited 50.0 %, 43.3 %, and 21.5 % higher compressive potency, respectively, than the cement without additives. The presence of DFNS@Chitosan in the cement mortar enhanced the adhesion between the coarse particles and paste, favorably affecting the physical characteristics of the interfacial transition zone. Additionally, the DFNS@Chitosan reduced capillary porosity, further contributing to the increased load-bearing capacity of the cement-based mortar. Fig. 10 illustrates the interfacial stretching potency of the cement-based mortars. It is evident that the interfacial stretching potency of all mortars increased with curing age. A significant improvement of interfacial stretching potency of 35.4 % and 32.2 % was observed for DFNS and DFNS@Chitosan, respectively, compared to the cement without additives at 5 days. The DFNS@Chitosan limited crack propagation via the bridging effect between DFNS@Chitosan and the cement matrix, thereby enhancing the stretching potency of the cement mortar. Additionally, chitosan support on the DFNS surface led to increased coarseness and improved interface adhesion with the cement matrix.

As cement continuously hydrated, the free water content in the cement matrix decreased slowly over time, leading to a reduction in water saturation within the pore structure. This process resulted in the formation of a broad spectrum of voids, ranging from nano to micro scale, in the hardened cement paste. The transition of tiny channels from a saturated to an unsaturated state led to the formation of concave surfaces within the tiny channels, generating internal pressure and subsequent autogenous shrinkage. Fig. 11 displays the results of assessments of the auto-induced deformation in the paste cases. The incorporation of DFNS and DFNS@Chitosan in the cement paste significantly mitigated autogenous shrinkage. This can be attributed to the complex three-dimensional system formed by

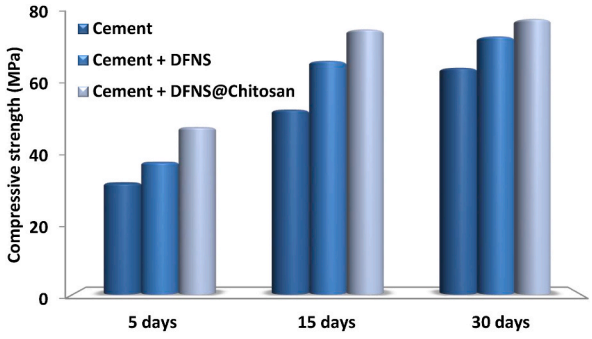

Fig. 9. The ability of mortars to bear loads with and without DFNS and DFNS@Chitosan at various stages of curing.

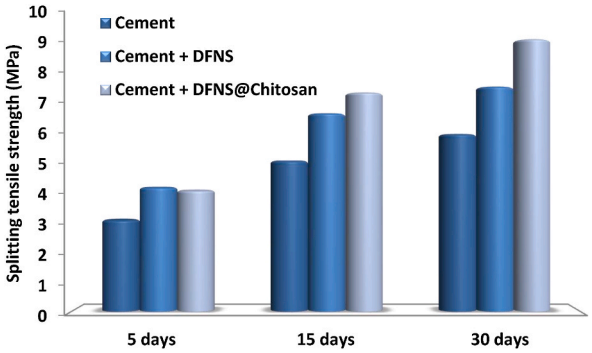

Fig. 10. Interfacial stretching potency of mortars with and without DFNS and DFNS@Chitosan at different curing ages.

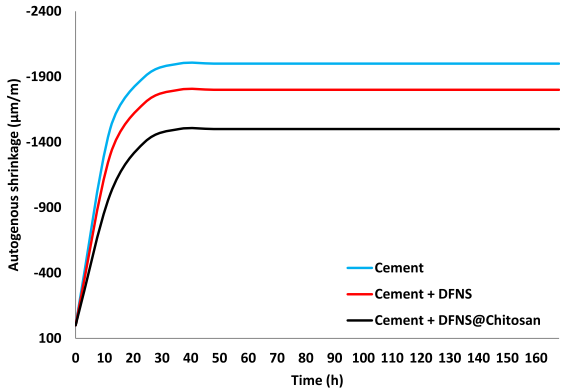

Fig. 11. The autogenous deformation curves of cement paste with and devoid DFNS and DFNS@Chitosan.

the random distribution of DFNS and DFNS@Chitosan within the cement paste. The existence of a water film adsorbed on the external level of DFNS and DFNS@Chitosan slowed down water overflow and hindered water loss, thus reducing autogenous shrinkage. Additionally, DFNS and DFNS@Chitosan, as natural hydrophilic fibers, had the capacity to absorb excess water in cement-based composites and discharge it via their distinctive porous arrangement as the external relative humidity diminishes.

4. Conclusions

The functionalization of DFNS using microcrystalline chitosan extracted from shrimp shells as a robust anchor was suggested for use in cement-based composites as a strengthening substance. The characteristics of DFNS@Chitosan were compared and evaluated using various techniques such as TEM, SEM, TGA, FTIR, AFM, XPS, and EDX. The study also investigated the effects of DFNS@Chitosan on the mechanical and auto-induced contraction properties of cement-based composites. The addition of DFNS@Chitosan was found to enhance the load-bearing capacity of cement-based mortar and the interfacial stretching potency, particularly evident when 2 % DFNS@Chitosan was included in the cement-based materials. Additionally, the inclusion of DFNS@Chitosan reduced the auto-induced contraction of cement paste. In summary, this study presents an alternative method for the recycling of chitosan from shrimp shells and highlights the practical value of the favorable utilization of DFNS@Chitosan in creating substances. Further investigation is necessary, particularly with regard to the practical application on a large scale, economic feasibility, and the advantages of the pretreatment methods and technology.

CRediT authorship contribution statement

Liyuan Zhao: Writing – original draft, Data curation, Conceptualization. **Man Wang:** Supervision, Resources, Methodology. **Liwei Zhang:** Validation, Methodology. **Seyed Mohsen Sadeghzadeh:** Writing – original draft, Formal analysis, Data curation.

Declaration of competing interest

The functionalization of DFNS using microcrystalline chitosan extracted from shrimp shells as a robust anchor was suggested for use in cement-based composites as a strengthening substance. The characteristics of DFNS@Chitosan were compared and evaluated

using various techniques such as TEM, SEM, TGA, FTIR, AFM, XPS, and EDX. The study also investigated the effects of DFNS@Chitosan on the mechanical and auto-induced contraction properties of cement-based composites. The addition of DFNS@Chitosan was found to enhance the load-bearing capacity of cement-based mortar and the interfacial stretching potency, particularly evident when 2 % DFNS@Chitosan was included in the cement-based materials. Additionally, the inclusion of DFNS@Chitosan reduced the auto-induced contraction of cement paste. In summary, this study presents an alternative method for the recycling of chitosan from shrimp shells and highlights the practical value of the favorable utilization of DFNS@Chitosan in creating substances. Further investigation is necessary, particularly with regard to the practical application on a large scale, economic feasibility, and the advantages of the pretreatment methods and technology.

Acknowledgments

Scientific and Technological Project of Henan Province (242102230023): Research on Key Technologies and axial Compression Properties of Large-diameter Composite Cylindrical Shells based on pultrusion/Winding Process.

References

[1] Y. Gong, Y. Wang, P. Li, Y. Yuan, F. Kong, J. CO2 Util. 79 (2024) 102656.
[2] S. Xie, Q. Qin, H. Liu, L. Jin, X. Wei, J. Liu, X. Liu, Y. Yao, L. Dong, B. Li, ACS Appl. Mater. Interfaces 12 (2020) 48476–48485.
[3] Z. Gao, L. Liang, X. Zhang, P. Xu, J. Sun, ACS Appl. Mater. Interfaces 13 (2021) 61334–61345.
[4] T.M. McDonald, W.R. Lee, J.A. Mason, B.M. Wiers, C.S. Hong, J.R. Long, J. Am. Chem. Soc. 134 (2012) 7056–7065.
[5] P.I. Scheurle, A. Mähringer, A.C. Jakowetz, P. Hosseini, A.F. Richter, G. Wittstock, D.D. Medina, T. Bein, Nanoscale 11 (2019) 20949–20955.
[6] S. Kundu, V. Polshettiwar, ChemPhotoChem 2 (2018) 796–800.
[7] A. Shaabani, M.B. Boroujeni, M.S. Laeini, RSC Adv. 6 (2016) 27706–27713.
[8] L. Carlsen, O.A. Kenesova, S.E. Batyrbekova, Chemosphere 67 (2007) 1108–1116.
[9] D.J. Neubaum, K.R. Wilson, T.J. O'shea, J. Wildl. Manag. 71 (2007) 728–736.
[10] C.M. DeLong, R. Bragg, J.A. Simmons, J. Acoust. Soc. Am. 123 (2008) 4582–4598.
[11] C. Chiu, C.F. Moss, J. Acoust. Soc. Am. 121 (2007) 2227–2235.
[12] Z.A. Zorina, T.A. Obozova, Zool. Zhurnal 90 (2011) 784–802.
[13] O.N. Fraser, T. Bugnyar, PLoS One 6 (2011) 18118.
[14] G. Lunn, E.B. Sansone, Chemosphere 29 (1994) 1577–1590.
[15] T.L. Varghese, S.C. Gaindhar, J. David, Defence Sci. J. 45 (1995) 25–30.
[16] N. Anbu, R. Maheswari, V. Elamathi, P. Varalakshmi, A. Dhakshinamoorthy, Catal. Commun. 138 (2020) 105954.
[17] E.A. Burns, E.A. Lawler, Aanl. Chem. 35 (1963) 802–806.
[18] N.J. Emery, Philos. Trans. R. Soc. Lond. B Biol. Sci. 361 (2006) 23–43.
[19] I.M. Pepperberg, A. Schachner, T.F. Brady, Curr. Biol. 19 (2009) 831–836.
[20] K.A. Bhaskaran, M.C. Gupta, T. Just, Combust. Flame 21 (1973) 45–48.
[21] M.S. Funk, Anim. Cognit. 5 (2002) 167–176.
[22] V. Polshettiwar, Acc. Chem. Res. 10 (2022) 1395–1410.
[23] R. Singh, N. Bayal, A. Maity, D.J. Pradeep, J. Trébosc, P.K. Madhu, O. Lafon, V. Polshettiwar, ChemNanoMat 4 (2018) 1231–1239.
[24] R. Singh, R. Bapat, L. Qin, H. Feng, V. Polshettiwar, ACS Catal. 6 (2016) 2770–2784.
[25] S. Kundu, V. Polshettiwar, ChemPhotoChem 2 (2018) 796–800.
[26] N. Bayal, R. Singh, V. Polshettiwar, ChemSusChem 10 (2017) 2182–2191.
[27] S.A. Rawool, Y. Karb, V. Polshettiwar, Mater. Adv. 3 (2022) 8449–8459.
[28] S.A. Rawool, A. Samanta, T.G. Ajithkumar, Y. Kar, V. Polshettiwar, ACS Appl. Energy Mater. 3 (2020) 8150–8158.
[29] R. Xiao, X. Jiang, Y. Wang, Q. He, B.S. Huang, J. mater Madani Engineer 33 (2021) 04021312.
[30] X. Jiang, R. Xiao, Y. Bai, B.S. Huang, Y.T. We, J. clean. Production (2022) 130778.
[31] X. Jiang, R. Xiao, Y.T. Ma, M.M. Zhang, Y. Bai, B.S. Huang, Construct. Build. Mater. 262 (2020) 120579.
[32] X. Jiang, R. Xiao, M.M. Zhang, W. Hu, Y. Bai, B.S. Huang, Construct. Build. Mater. 254 (2020) 119267.